

Brillouin gain spectrum dependence on large strain in perfluorinated graded-index polymer optical fiber

Neisei Hayashi,* Yosuke Mizuno, and Kentaro Nakamura

Precision and Intelligence Laboratory, Tokyo Institute of Technology, 4259 Nagatsuta-cho, Midori-ku, Yokohama 226-8503, Japan

*hayashi@sonic.pi.titech.ac.jp

Abstract: We investigate the dependence of Brillouin gain spectra on large strain of $> 20\%$ in a perfluorinated graded-index polymer optical fiber, and prove, for the first time, that the dependence of Brillouin frequency shift (BFS) is highly non-monotonic. We predict that temperature sensors even with zero strain sensitivity can be implemented by use of this non-monotonic nature. Meanwhile, the Stokes power decreases rapidly when the applied strain is $> \sim 10\%$. This behavior seems to originate from the propagation loss dependence on large strain. By exploiting the Stokes power dependence, we can probably solve the problem of how to identify the applied strain, when the identification is difficult only by BFS because of its non-monotonic nature.

©2012 Optical Society of America

OCIS codes: (160.5470) Polymers; (280.4788) Optical sensing and sensors; (290.5830) Scattering, Brillouin.

References and links

1. T. Horiguchi and M. Tateda, "BOTDA—nondestructive measurement of single-mode optical fiber attenuation characteristics using Brillouin interaction: theory," *J. Lightwave Technol.* **7**(8), 1170–1176 (1989).
2. T. Kurashima, T. Horiguchi, H. Izumita, and M. Tateda, "Brillouin optical-fiber time domain reflectometry," *IEICE Trans. Commun.* **E76-B**, 382–390 (1993).
3. D. Garus, K. Krebber, F. Schliep, and T. Gogolla, "Distributed sensing technique based on Brillouin optical-fiber frequency-domain analysis," *Opt. Lett.* **21**(17), 1402–1404 (1996).
4. K. Hotate and T. Hasegawa, "Measurement of Brillouin gain spectrum distribution along an optical fiber using a correlation-based technique – Proposal, experiment and simulation," *IEICE Trans. Electron.* **E83-C**, 405–412 (2000).
5. Y. Mizuno, W. Zou, Z. He, and K. Hotate, "Proposal of Brillouin optical correlation-domain reflectometry (BOCDR)," *Opt. Express* **16**(16), 12148–12153 (2008).
6. M. G. Kuzyk, *Polymer Fiber Optics: Materials, Physics, and Applications* (CRC Press, 2006).
7. K. Nakamura, I. R. Husdi, and S. Ueha, "A distributed strain sensor with the memory effect based on the POF OTDR," *Proc. SPIE* **5855**, 807–810 (2005).
8. N. Hayashi, Y. Mizuno, D. Koyama, and K. Nakamura, "Measurement of acoustic velocity in poly(methyl methacrylate)-based polymer optical fiber for Brillouin frequency shift estimation," *Appl. Phys. Express* **4**(10), 102501 (2011), doi:10.1143/APEX.4.102501.
9. N. Hayashi, Y. Mizuno, D. Koyama, and K. Nakamura, "Dependence of Brillouin frequency shift on temperature and strain in poly(methyl methacrylate)-based polymer optical fibers estimated by acoustic velocity measurement," *Appl. Phys. Express* **5**(3), 032502 (2012), doi:10.1143/APEX.5.032502.
10. Y. Mizuno and K. Nakamura, "Experimental study of Brillouin scattering in perfluorinated polymer optical fiber at telecommunication wavelength," *Appl. Phys. Lett.* **97**(2), 021103 (2010), doi:10.1063/1.3463038.
11. Y. Mizuno, M. Kishi, K. Hotate, T. Ishigure, and K. Nakamura, "Observation of stimulated Brillouin scattering in polymer optical fiber with pump-probe technique," *Opt. Lett.* **36**(12), 2378–2380 (2011).
12. Y. Mizuno, T. Ishigure, and K. Nakamura, "Brillouin gain spectrum characterization in perfluorinated graded-index polymer optical fiber with 62.5- μm core diameter," *IEEE Photon. Technol. Lett.* **23**(24), 1863–1865 (2011).
13. Y. Mizuno and K. Nakamura, "Potential of Brillouin scattering in polymer optical fiber for strain-insensitive high-accuracy temperature sensing," *Opt. Lett.* **35**(23), 3985–3987 (2010).
14. G. P. Agrawal, *Nonlinear Fiber Optics* (Academic Press, 1995).

15. T. Horiguchi, T. Kurashima, and M. Tateda, "Tensile strain dependence of Brillouin frequency shift in silica optical fibers," *IEEE Photon. Technol. Lett.* **1**(5), 107–108 (1989).
 16. Y. Mizuno, Z. He, and K. Hotate, "Distributed strain measurement using a tellurite glass fiber with Brillouin optical correlation-domain reflectometry," *Opt. Commun.* **283**(11), 2438–2441 (2010).
 17. L. Zou, X. Bao, S. Afshar V, and L. Chen, "Dependence of the Brillouin frequency shift on strain and temperature in a photonic crystal fiber," *Opt. Lett.* **29**(13), 1485–1487 (2004).
 18. M. Nikles, L. Thevenaz, and P. A. Robert, "Brillouin gain spectrum characterization in single-mode optical fibers," *J. Lightwave Technol.* **15**(10), 1842–1851 (1997).
 19. O. Frank and J. Lehmann, "Determination of various deformation processes in impact-modified PMMA at strain rates up to $10^5\%/min$," *Colloid Polym. Sci.* **264**(6), 473–481 (1986).
 20. R. Hill, *The Mathematical Theory of Plasticity* (Oxford U. Press, 1950).
-

1. Introduction

Due to their light weight, small diameter, immunity against electro-magnetic noise, etc., optical fiber sensors have been increasingly required for monitoring diverse civil structures, such as buildings, dams, levees, bridges, pipelines, tunnels, and aircraft wings. Above all, Brillouin scattering-based fiber-optic sensors have been extensively studied because they can measure strain/temperature distribution along the fibers [1–5]. Up to now, only glass optical fibers (GOFs) have been used for their sensor heads, but they are quite fragile and cannot withstand strains of over several %. As one way to solve this problem, employing polymer optical fibers (POFs) in such Brillouin sensors has attracted considerable attention, which has extremely high flexibility and can withstand $> 50\%$ strain [6]. Besides, POFs have a unique feature called the "memory effect" [7], with which the information on the applied large strain can be stored due to their plastic deformation.

Commercially-available POFs are classified into two types: poly(methyl methacrylate)-based (PMMA-) POFs and perfluorinated graded-index (PFGI-) POFs. The former mainly transmit visible light at around 650 nm, whereas the latter transmit not only visible light but also telecom wavelength light at up to 1.55 μm . Brillouin scattering in PMMA-POFs has not been experimentally observed yet, because some of the optical devices required for the measurement are extremely difficult to prepare at visible wavelength. Therefore, we have developed a method to characterize the Brillouin properties in POFs using a so-called ultrasonic pulse-echo technique [8], and predicted that the strain dependence on Brillouin frequency shift (BFS) in PMMA-POFs is non-monotonic when applied strain is larger than $\sim 10\%$ [9]. Meanwhile, Brillouin scattering in PFGI-POFs has already been experimentally observed, since various optical devices are available at telecom wavelength [10–13]. The BFS dependence on strain in PFGI-POFs has been measured to be linear with a coefficient of -121.8 MHz/%, but, in our previous experiment, the applied strain ranged merely from 0% to 0.8% [13]. Putting their memory effect in perspective, the BFS dependence on large strain in PFGI-POFs needs to be clarified.

In this study, we experimentally investigate the dependence of Brillouin gain spectra (BGS) on large strain of up to 20% in a PFGI-POF. The BFS dependence is found to be non-monotonic, which agrees with our prediction concerning PMMA-POFs [8]. By exploiting this non-monotonic nature, temperature sensing even with zero strain sensitivity will be feasible. As for the Stokes power, it is found to decrease drastically when the applied strain is larger than 10%. We show that this behavior is well explained by the propagation loss dependence on large strain. Utilizing the Stokes power dependence is one way to solve the problem of how we should identify the applied strain, when it is difficult only by BFS due to its non-monotonic nature.

2. Principle

When a light beam is propagating in an optical fiber, it interacts with acoustic phonons and generates a backscattered light beam called the Stokes light [14]. This phenomenon is known as Brillouin scattering, and the Stokes light spectrum is called the BGS. The center frequency

of the BGS is known to be down-shifted from that of the incident light; the amount of this frequency shift ν_B , called the BFS, is given as

$$\nu_B = \frac{2n\nu_A}{\lambda}, \quad (1)$$

In Eq. (1), n is the refractive index, ν_A is the acoustic velocity in the fiber, and λ is the wavelength of the incident light.

If strain (or temperature change) is applied to the fiber, the BFS shifts toward higher or lower frequency depending on the fiber core material, which is the basic principle of fiber-optic Brillouin sensors. The BFS dependence on strain has been investigated for a variety of optical fibers. They include silica single-mode fibers (SMFs) [15], tellurite glass fibers [16], germanium-doped photonic crystal fibers (PCFs) [17], and PFGI-POFs [13], the strain coefficients of which are reported to be + 580, -230, + 409 (main peak), and -122 MHz/%, respectively. Here, we should note that the value for the PFGI-POF is valid only for strain of $< \sim 1\%$.

As well as the BFS, the Stokes power is also strain-dependent; for instance, the Stokes power in silica SMFs is known to decrease with the increasing strain [18]. The Stokes power (or the Brillouin gain coefficient) is a function of many structural quantities [14], one of which is the effective length L_{eff} defined as

$$L_{\text{eff}} = \frac{1 - e^{-\alpha L}}{\alpha}, \quad (2)$$

where α is propagation loss and L is the fiber length.

3. Experimental setup

We employed a 1.27-m-long PFGI-POF as a fiber under test (FUT), which had numerical aperture (NA) of 0.185, core diameter of 50 μm , cladding diameter of 750 μm , core refractive index of ~ 1.35 , and propagation loss of ~ 250 dB/km at 1.55 μm . The experimental setup for investigating the BFS dependence on large strain in the PFGI-POF was basically the same as that previously reported in [10], where the BGS can be observed with a high resolution (3 MHz in this experiment) by self-heterodyne detection. One end of the PFGI-POF was butt-coupled to a silica SMF via an SC connector, and the other end was guided to an optical power-meter. Polarization state was adjusted for each measurement with polarization controllers so that the Stokes power may be maximal. Different strains of up to 20% were applied to the whole length of the PFGI-POF fixed on two translation stages. The temperature was kept at 27 $^{\circ}\text{C}$ for all the measurements.

4. Experimental results

Figure 1 shows a stress-strain curve of a 0.1-m PFGI-POF of the identical type, which was obtained with the same method (strain-applying speed: 100 mm/min) as in Ref [9]. The cross-sectional area was assumed to be constant during the measurement. Fracture strain of the PFGI-POF was 71% and its elastic-plastic transition was apparently induced at several % strain [19]. The initial peak up to $\sim 10\%$ indicates the elastic-to-plastic transition [20].

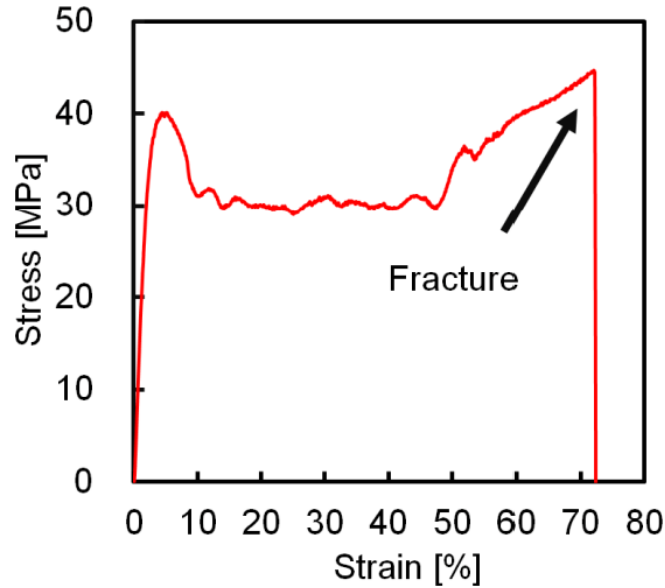


Fig. 1. Measured stress-strain curve of the PFGI-POF.

The measured BGS dependence on large strain of up to 18.3% in the PFGI-POF is shown in Fig. 2(a). It took tens of seconds to manually apply a specific strain to the PFGI-POF; then, a few minutes later, the BGS measurement was performed. When the strain was 2.6%, a small peak was clearly observed at approximately 2.8 GHz. This peak was caused by a 6-cm portion of the PFGI-POF end connected to the silica SMF, to which proper strain was not applicable. From this measurement, the dependences of the BFS and the Stokes power on large strain can be plotted as shown in Figs. 2(b) and (c), respectively. In Fig. 2(b), the BFS dependence on strain was non-monotonic; with the increasing strain, the BFS shifted at first toward lower frequency (0-2.6%) (this shift agrees well with the result under small strain [13]), then toward higher frequency (2.6-8.1%), and finally became almost constant (8.1-18.3%). This behavior may be caused by the Young's modulus dependence on large strain [13]. In Fig. 2(c), with the increasing strain, the Stokes power decreased, and its reduction grew drastic when the strain was over ~10%. At ~20% strain, the Stokes power became so low that the target BGS was buried by the noise, i.e., by the BGS of the small portion of the PFGI-POF without strain applied. The fluctuations in the Stokes power were caused by the unstable polarization state. The dependence of the Brillouin linewidth on large strain is also a significant property, but we did not evaluate it because the Stokes power was so small that its fair measurement was not feasible. The repeatability of the results above has been confirmed by performing the same measurements for other samples.

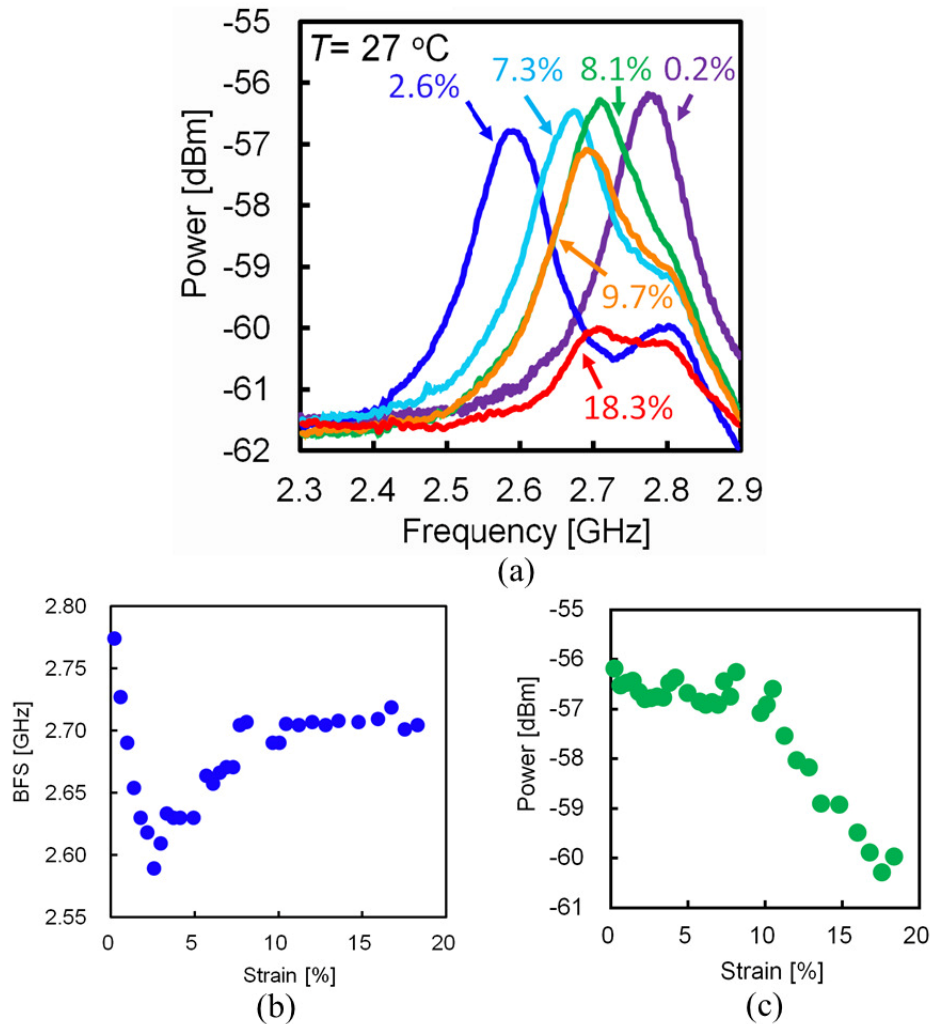


Fig. 2. Measured large-strain dependences of (a) the BGS, (b) the BFS, and (c) the Stokes power in the PFGI-POF.

To clarify the origin of the Stokes power dependence on strain given in Fig. 2(c), the propagation loss was also measured as a function of strain as shown in Fig. 3(a). The loss drastically increased when the strain was over $\sim 10\%$. Then, based on this figure, the strain dependence of the effective length was calculated using Eq. (2), which is given in Fig. 3(b). With the increasing strain, the effective length started to decrease drastically when the strain was over $\sim 10\%$, which is in good agreement with the Stokes power dependence. In Fig. 3(b), when the strain was smaller than 5%, the effective length was slightly increased with the strain, because the actual fiber length was elongated owing to the strain and it compensated for the increase in the loss. This behavior is different from that in the Stokes power dependence in Fig. 2(c), but it is valid if we consider that the small peak at ~ 2.8 GHz caused by the small portion of the PFGI-POF was overlapped with the target BGS at such small strains. Thus, we presume that the reduction of the Stokes power in the PFGI-POF with strain is attributed to that of the propagation loss.

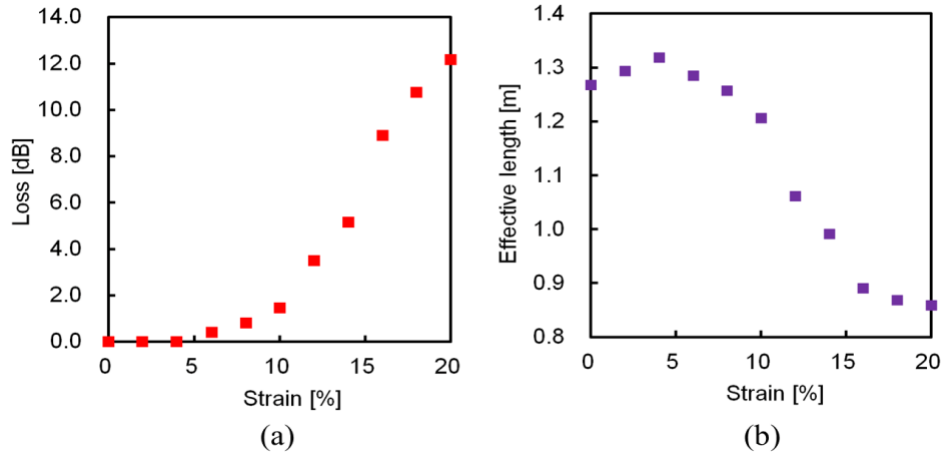


Fig. 3. Measured large-strain dependences of (a) the propagation loss and (b) the effective length in the PFGI-POF.

By exploiting these unique Brillouin features of PFGI-POFs, some useful devices and systems will be developed. For instance, the BFS in a PFGI-POF to which 10-15% strain is applied has no strain dependence, and consequently it may be used for temperature sensing with almost zero strain sensitivity. We must note that, due to the non-monotonic nature of BFS, the identification of the applied large strain is sometimes difficult only by BFS. We may solve this problem by applying $\sim 2.6\%$ strain beforehand and/or by using the Stokes power dependence on strain as well.

5. Conclusion

By applying large strain of up to 20%, the strain dependence of BGS in the PFGI-POF was measured in detail. The BFS exhibited a non-monotonic nature, with which temperature sensing even with zero strain sensitivity will be feasible. The Stokes power drastically dropped when the applied strain was larger than $\sim 10\%$. This behavior is probably caused by the large-strain dependence of the propagation loss. The identification of the applied strain is sometimes difficult only by BFS due to its non-monotonic nature; in that case, using the Stokes power dependence will be one of the solutions. Since this nature may vary depending on the time of applying strain or the types of the POFs (PMMA-POFs, partially-chlorinated POF, etc.), further investigation is required on this point. We believe that these results are of great significance in developing large-strain sensors based on Brillouin scattering in POFs.

Acknowledgments

We are indebted to Professor Hosoda and Ms. Naruse of Tokyo Institute of Technology, Japan, for instructing us in the use of the tension tester. This work was partially supported by the Research Fellowships for Young Scientists from the Japan Society for the Promotion of Science (JSPS), and by research grants from the Murata Science Foundation and the Foundation of Ando Laboratory.